Materials Advances

ROYAL SOCIETY OF CHEMISTRY

PAPER

View Article Online
View Journal | View Issue

Cite this: *Mater. Adv.*, 2022, 3, 4342

Ratiometric electrochemical detection of tryptophan based on ferrocene and carboxylated-pillar[6]arene hybrid metal–organic layers†

Zejia Wu,[a] Jia Wen,*[b] Jiangshan Li,[a] Wuyi Zhang,[b] Yutong Li,[a] Wei Li*[a] and Kui Yang*[a]

Metal–organic layers (MOLs), which have an ultrathin structure, are a novel class of two dimensional coordination polymers. In comparison with three dimensional metal–organic frameworks, MOLs have more accessible active sites on the surfaces and better electron transfer efficiency. These advantages endow MOLs with great potential for the construction of multifunctional nano-platforms, especially electrochemical sensing platforms. In this study, a ratiometric electrochemical sensing platform based on functionalized Zr-MOL was designed and constructed. Ferrocenecarboxylic acid (Fc) was modified on the surface of Zr-MOL on the basis of the solvent-assisted ligand incorporation method, thus obtaining Fc-MOL. Then, carboxylated-pillar[6]arene (WP6) was assembled on the surface of Fc-MOL on the basis of the coordination interaction between bare metal joints and carboxyl groups. The as-prepared hybrid materials WP6@Fc-MOL were characterized by powder X-ray diffraction, transmission electron microscopy, energy dispersive spectroscopy mapping, and inductively coupled plasma-optical emission spectroscopy. With the use of the host–guest interaction between WP6 and tryptophan (Trp), WP6@Fc-MOL exhibited high selectivity for Trp sensing. In addition, Fc, as the interior label, can not only reduce the interference of other factors but also increase the electron transfer efficiency during sensing. Results demonstrate that the R^2 of linear fitting of the single-signal method and the ratiometric method was 0.9777 and 0.9958, respectively. Benefiting from the advantages of the ratiometric detection method, WP6@Fc-MOL showed improved stability and accuracy for Trp sensing.

Received 4th February 2022,
Accepted 13th April 2022

DOI: 10.1039/d2ma00125j

rsc.li/materials-advances

Introduction

Bioactive small molecules, such as amino acids,[1] dopamine,[2] nucleotides,[3] and glucose,[4] particularly those that are related to disease diagnosis, play important roles in the human body. The detection and quantitative analysis of bioactive small molecules are essential for life sciences and biomedicine. Tryptophan (Trp), which plays roles as nutrition and antioxidant in the body, is an essential amino acid.[5] The disorder of Trp metabolism may be closely related to Alzheimer's disease and cancer.[6] Thus, the detection of Trp is significant. Electrochemical sensing based on the redox changes of electrode surfaces is becoming a highly favored method for small molecule detection because of its convenience. However, the accuracy and repeatability of general electrochemical sensing depending on single-signal output may be influenced by environment conditions and operation process. For example, Zhang's group reported that the relative standard deviations (RSDs) of single-signal sensor constructed from β-cyclodextrin (β-CD) or prussian blue (PB) is not as low as that of the ratiometric electrochemical sensor constructed based on β-CD and PB for imidacloprid sensing.[7] In addition, they found that the ratiometric electrochemical analysis could also improve the longterm stability of the sensor. Consequently, the ratiometric strategy could effectively reduce the interferences from internal or external factors and improve the robustness and precision of detections. To solve this problem, ratiometric electrochemical sensing has been developed for stable and accurate measurement.[8,9] A multifunctional electrode material is highly preferred to construct ratiometric electrochemical sensors.

Metal–organic frameworks (MOFs) are composed of organic ligands and metal nodes, which have been widely used in

[a] *Key Laboratory of Medicinal Chemistry and Molecular Diagnosis of the Ministry of Education, Key Laboratory of Chemical Biology of Hebei Province, College of Chemistry and Environmental Science, Hebei University, Baoding 071002, P. R. China. E-mail: yangkuihbu@126.com, liweihebeilab@163.com*

[b] *Key Laboratory of Pharmaceutical Quality Control of Hebei Province, College of Pharmaceutical Science, Hebei University, Baoding 071002, China. E-mail: wenjiahbu@163.com*

† Electronic supplementary information (ESI) available. See DOI: https://doi.org/10.1039/d2ma00125j

diverse fields, including catalysis,[10,11] energy,[12,13] gas separation,[14] sensing,[15] and biomedicine.[16] Metal–organic layers (MOLs), as a part of MOFs, are monolayer or a few layers.[17] Benefiting from their two-dimensional and ultrathin structure, MOLs can provide more accessible active sites during the catalysis or sensing process and exhibit excellent electron transfer efficiency, and they have been used in photocatalysis,[18,19] electrocatalysis, sensing,[20] and nanomedicine.[21] In addition, MOLs, as a type of ultrathin two-dimensional material, can provide more active sites to combine with functional molecules[22,23] or other nanomaterials,[24,25] which show great potential for the construction of multifunctional electrode materials.

Pillar[*n*]arenes, which possess a rigid structure and electron-rich cavity, are a novel generation of macrocycles.[26,27] Electrochemical applications based on pillar[*n*]arenes have been well developed in the last decade for improving electrode interface amphiphilicity and electron transfer efficiency.[28] For example, a hybrid nanocomposite based on amphiphilic pillar[5]arene, gold nanoparticles, and reduced graphene has been developed as an electrode material.[29] With its rigid pillar structures and electron-donating cavities of pillar[5]arene, the hybrid nanocomposite showed high electrochemical response toward guest molecules such as dopamine. Even though many relevant works have been conducted, a ratiometric electrochemical sensing platform based on pillar[*n*]arenes has been rarely reported.

In this study, a ratiometric electrochemical sensing platform based on carboxylated-pillar[6]arene (WP6) and ferrocenecarboxylic acid (Fc) functionalized Zr-MOL was designed and constructed for Trp detection. The Fc, which was used as internal electrical signal, was modified on the surface of Zr-MOL based on the solvent-assisted ligand incorporation method, which obtains Fc-MOL.[30] Then, WP6 was assembled on the surface of Fc-MOL based on the coordination interaction between bare metal joints of MOL and carboxyl groups of WP6.[31] The obtained WP6@Fc-MOL can be used as a multifunctional electrode material for the ratiometric electrochemical detection of Trp (Scheme 1).

Results and discussion

Preparation and characterization of WP6@Fc-MOL

Zr-MOL and WP6 were synthesized according to previous literature.[32,33] WP6 was confirmed by NMR (Fig. S1 in the ESI†). Then, the structures of MOL, Fc-MOL, and WP6@Fc-MOL were characterized in detail by different methods. The transmission electron microscopy (TEM) results in Fig. 1(a) and Fig. S2 (ESI†) showed that MOL, Fc-MOL, and WP6@Fc-MOL are lamellar structures. The energy dispersive spectroscopy-mapping results indicate the uniform distribution of C, O, Fe, and Zr in WP6@Fc-MOL, which demonstrates the successful assembly of WP6@Fc-MOL (Fig. 1(b)). Atomic force microscopy (AFM) was used to calculate the thickness of Zr-MOL. The result in Fig. 1(c) shows that the thickness of Zr-MOL was about 1.8 nm, which was similar to the previous literature.[34] Thus, the as-prepared MOL was almost monolayer. The powder X-ray

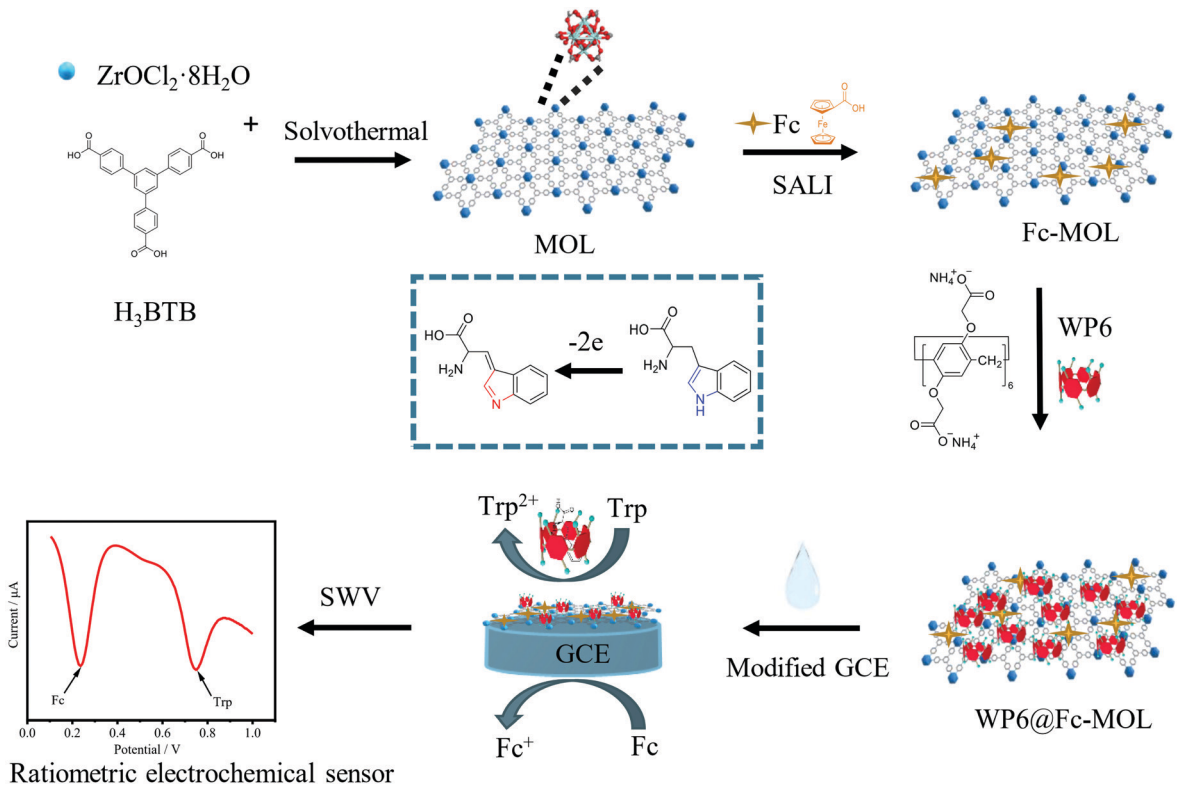

Scheme 1 Schematic illustration of a ratiometric electrochemical sensing platform based on WP6 and Fc functionalised Zr-MOL for Trp detection.

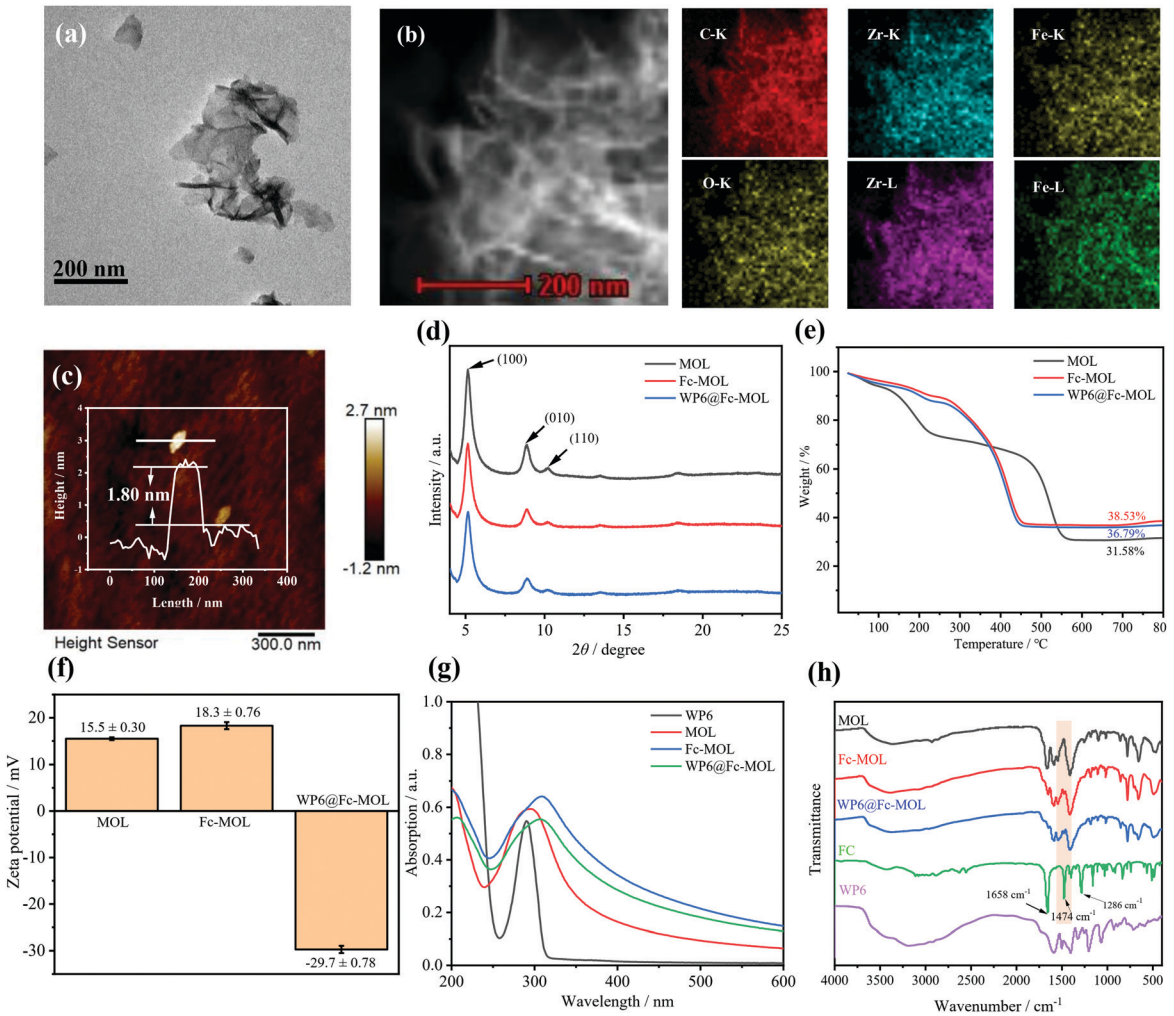

Fig. 1 (a) TEM image of WP6@Fc-MOL. (b) Elemental mapping images of WP6@Fc-MOL. (c) Tapping-mode AFM topography of MOL, the height profile along the white line of MOL. (d) PXRD patterns of MOL, Fc-MOL and WP6@Fc-MOL. (e) Thermogravimetric analysis of MOL, Fc-MOL and WP6@Fc-MOL. (f) Zeta potential values of MOL, Fc-MOL and WP6@Fc-MOL. (g) UV-vis spectra of WP6, MOL, Fc-MOL and WP6@Fc-MOL. (h) FT-IR spectra of MOL, Fc-MOL, WP6@Fc-MOL, Fc and WP6.

diffraction (PXRD) results in Fig. 1(d) demonstrate that the characteristic peaks of Zr-MOL including (100), (010), and (110), also existed in Fc-MOL and WP6@Fc-MOL, indicating that Fc-MOL and WP6@Fc-MOL still remained the crystal form of Zr-MOL.[34] The TGA results showed that the residual mass of metal oxides was increased when adding Fc in the hybrid materials. This was because the residual components of Fc were metal oxides. This result proved the assembly of Fc. While when WP6 was assembled on the surface of Fc-MOL, the residual mass was decreased slightly owing that WP6 was organic compound. The slight decrease of residual mass demonstrated that WP6 was assembled on Zr-MOL successfully. In the FTIR results, the characteristic peaks of Fc,[35] including 1286 cm^{-1}, 1474 cm^{-1} and 1658 cm^{-1}, were founded in the Fc-MOL and WP6@Fc-MOL, indicating that Fc was assembled on Zr-MOL successfully. The zeta potential result of WP6@Fc-MOL in aqueous solution was -29.7 ± 0.78 mV, which meant that WP6@Fc-MOL was stable in water (Fig. 1(f)). In addition, the zeta potential of WP6@Fc-MOL was around -30 mV to -20 mV in phosphate buffered solution (PBS) with different pH values (Fig. S3, ESI†), thereby indicating the applicability of WP6@Fc-MOL. Inductively coupled plasma-optical emission spectroscopy (ICP-OES) was used to analyze the composition of WP6@Fc-MOL quantitatively. The results showed that the amount of Fe and Zr in WP6@Fc-MOL was about 3.18% and 19.17% separately (Table S1, ESI†).

Host–guest interaction between WP6 and Trp

The host–guest interaction between WP6 and Trp was explored using UV-vis spectra and NMR spectra. As shown in Fig. 2 and Fig. S4 (ESI†), the signals of Trp shifted upfield slightly. This result demonstrates the inclusion of Trp into the cavity of WP6, which was consistent with previous literature.[36] The best stoichiometry between WP6 and Trp was examined by applying Job's plot method based on UV-vis spectra, indicating that the best complex ratio was 1 : 1 (Fig. S5a and b, ESI†).

Electrochemical characterization of modified electrodes

The detailed preparation methods of modified electrodes are shown in the ESI.† Cyclic voltammetry (CV) and electrochemical impedance spectroscopy (EIS) measurements were

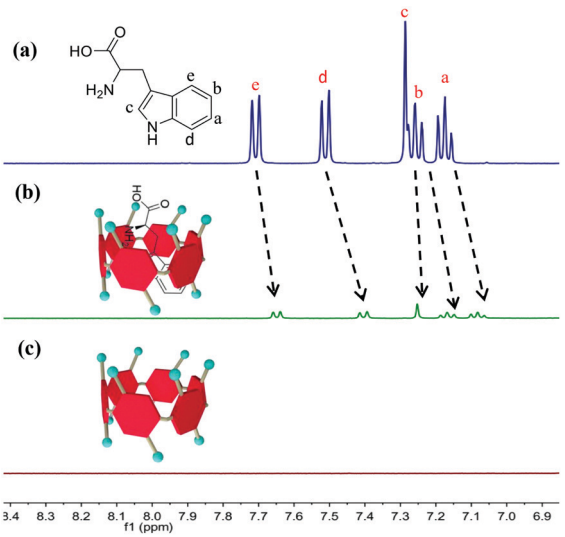

Fig. 2 ^{1}H NMR spectra (400 MHz, D_2O) of (a) 4.5 mM Trp, (b) 4.5 mM Trp + 4.5 mM WP6 and (c) 4.5 mM WP6.

implemented to monitor the conductivity and resistivity of different modified electrodes, including bare GCE, Nafion/GCE, Nafion/MOL/GCE, Nafion/Fc-MOL/GCE, and Nafion/WP6@Fc-MOL/GCE. First, CV of different modified electrodes were conducted in 5 mM $Fe(CN)_6^{3-/4-}$ containing 0.1 M KCl solution at a scan rate of 50 mV s^{-1} from −0.2 V to 0.6 V. As shown in Fig. 3(a), bare GCE displayed standard redox peaks of $Fe(CN)_6^{3-/4-}$. The redox current on Nafion/GCE and Nafion/MOL/GCE decreased relative to that on the bare GCE because Nafion and Zr-MOL hindered the interfacial electron transfer. However, when the electrode was modified with Nafion/Fc-MOL/GCE, the redox current increased obviously because of the excellent conductivity and electron transfer ability of Fc. Then, the redox current declined when Nafion/WP6@Fc-MOL/GCE was modified on the electrode. On the one hand, WP6 molecules with a negative charge would repulse $Fe(CN)_6^{3-/4-}$. On the other hand, WP6 with hydrophobic cavity cannot recognize ions. Therefore, WP6 would prevent electron transfer between electrode and $Fe(CN)_6^{3-/4-}$. Fig. 3(b) shows the results of EIS on different modified electrodes in the presence of equivalent 5.0 mM $Fe(CN)_6^{3-/4-}$ containing 0.1 M KCl solution. The GCE showed the lowest charge transfer resistance (R_{ct}) (148.3 Ω). For Nafion/GCE and Nafion/MOL/GCE, the R_{ct} value was 18 700 Ω and 3614 Ω, respectively, because of the obstruction of interfacial electron transfer of Nafion and Zr-MOL. However, when Fc was introduced on the surface of the modified electrode, the value of R_{ct} (823.6 Ω) was lower than that on Nafion/MOL/GCE because of the excellent conductivity and electron transfer ability of Fc. This result also indicates the successful preparation of Nafion/Fc-MOL/GCE modified electrodes. Nafion/WP6@Fc-MOL/GCE showed the largest R_{ct} (3811 Ω) mainly attributed to nonconducting WP6 molecules modified on the electrode, resulting in the increased resistance of modified electrodes. Therefore, EIS further confirmed the interfacial properties of different modified electrodes.

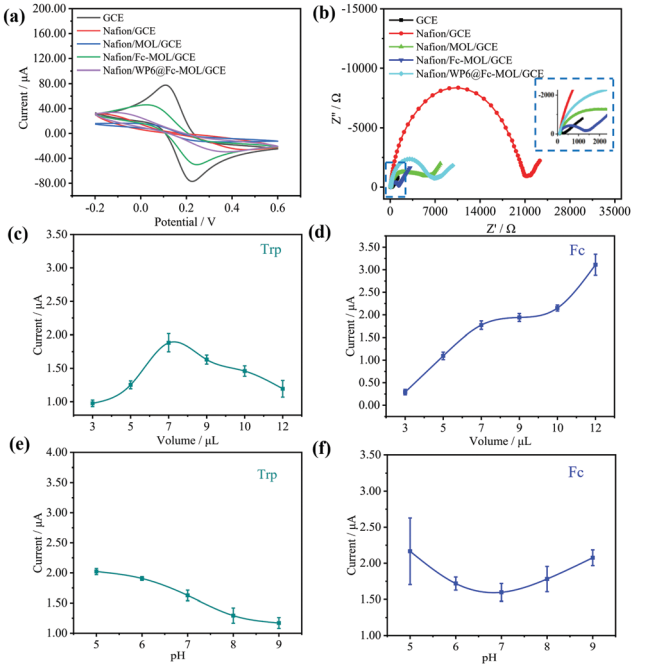

Fig. 3 (a) CV and (b) EIS responses of different electrodes characterized in 5 mM $[Fe(CN)_6]^{3-/4-}$ solution containing 0.1 M KCl. Signal response of 0.1 M PBS (pH = 6.0) tryptophan containing 50 μM Trp (c) and (d) at different drip coating levels and (e) and (f) different pH conditions.

Optimization of experimental conditions

The modified amount of WP6@Fc-MOL and pH values were investigated by current peaks of square wave voltammetry (SWV) method. The amount of WP6@Fc-MOL suspension increased from 3 μL to 12 μL. When this amount increased, the signal of Fc increased (Fig. 3(d)). When the amount was 7 μL, the Trp obtained the best signal (Fig. 3(c)). As a result, 7 μL was chosen as the amount of drip. The screening of pH was applied for the optimization of experimental conditions, and pH values from 5 to 9 of PBS were prepared. When the pH increased, the signal responses of Trp decreased (Fig. 3(e)). The signal responses of Fc increased first and then decreased when the pH values were higher than 7 (Fig. 3(f)). Considering the different factors, pH value 6 was chosen as the final detection condition.

Analytical performances of ratiometric electrochemical sensing platform

CV responses of Nafion/WP6@Fc-MOL/GCE at different scan rates ranging from 25 mV s^{-1} to 200 mV s^{-1} were carried out. The results in Fig. 4(a) show that the peak currents of Nafion/WP6@Fc-MOL/GCE shifted toward the positive potential range. The linear relationship between scan rates and current response was expressed as $y = 0.183x + 0.910$ with $R^2 = 0.9970$. These results indicate that the electrochemical oxidation progress of Trp based on WP6@Fc-MOL was the diffusion controlled process.

The response to Trp was also conducted at different modified electrodes, including GCE, Nafion/GCE, Nafion/MOL/GCE,

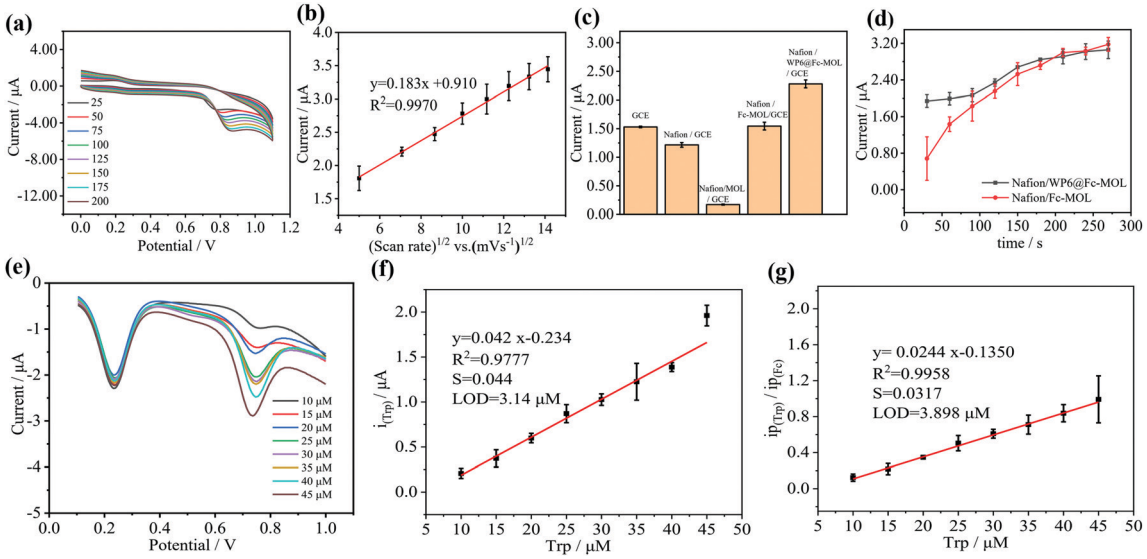

Fig. 4 (a) CV responses of Nafion/WP6@Fc-MOL/GCE at different scan rates (25–200 mV s^{-1}) in 0.1 M PBS (pH = 6.0) containing 50 μM Trp and (b) fitted curves of current response *versus* scan rates. (c) SWV responses of different electrodes in 0.1 M PBS (pH = 6.0) containing 50 μM Trp. (d) SWV responses of Nafion/FC-MOL/GCE and Nafion/WP6@Fc-MOL/GCE in 0.1 M PBS (pH = 6.0) containing 50 μM Trp for different time. (e) SWV responses of Trp from 10 μM to 45 μM in 0.1 M PBS (pH = 6.0) at Nafion/WP6@Fc-MOL/GCE. (f) The calibration plot of peak current ($ip_{(Trp)}$) *versus* concentration. (g) The calibration plot of peak current ($ip_{(Trp)}/ip_{(Fc)}$) *versus* concentration.

Nafion/Fc-MOL/GCE, and Nafion/WP6@Fc-MOL/GCE by SWV. The results in Fig. 4(c) show that the Nafion/WP6@Fc-MOL/GCE had the best current response of around 2.25 μA.

Adsorption time is an important parameter for detection. A comparison was conducted between WP6@Fc-MOL and Fc-MOL. The results in Fig. 4(d) indicate that WP6 contributed to the adsorption of Trp on the face of electrons in a short time, which was attributed to the host–guest interaction between WP6 and Trp.

The electrochemical sensing performance of Nafion/WP6@Fc-MOL/GCE toward Trp determination was investigated by SWV under optimum conditions. The results in Fig. 4(e) show that the current response values of Fc remained almost unchanged when the concentrations of Trp changed. The linear relationship equation based on a single signal of Trp was $y = 0.042x - 0.234$ with 0.9777 R^2 value (Fig. 4(f)). When the results were output by the ratiometric electrochemical method, the linear relationship equation was $y = 0.0244x - 0.1350$ with 0.9958 R^2 value (Fig. 4(g)). The detection limit showed no obvious difference, whereas the R^2 values increased obviously, thereby indicating the stability and accuracy of the ratiometric electrochemical method.

Some typical biomolecules, including lactose, L-cysteine, arabinose, fructose, and ascorbic acid were prepared for the interference study. The results in Fig. 5(a) illustrate the good anti-interference capability of Nafion/WP6@Fc-MOL/GCE. The repeatability assay was evaluated by five independent Nafion/WP6@Fc-MOL/GCE. The results in Fig. 5(b) also demonstrate the good reproducibility of Nafion/WP6@Fc-MOL/GCE with RSDs around 2.88%.

Real sample analysis

To evaluate the practicability of the ratiometric electrochemical sensing platform, milk samples were prepared for the analysis.

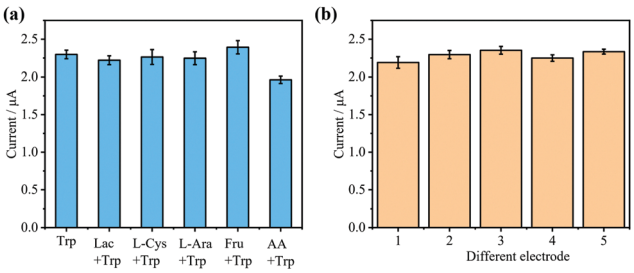

Fig. 5 (a) SWV responses of Trp and Trp containing excess other potential interfering biomolecules at Nafion/WP6@Fc-MOL/GCE. (b) Current responses of 5 independent Nafion/WP6@Fc-MOL/GCE in 0.1 M PBS (pH 6.0) containing 50 μM Trp. RSD = 2.88% (n = 5).

The concentrations of Trp in milk solutions were 20 and 30 μM. The response currents for Trp containing milk solutions were recorded by SWV. The results in Table 1 show that the corresponding concentrations obtained through the linear fitting equation were 21.6 ± 0.54 and 31.2 ± 1.21 μM. The recovery values were 108.25 ± 2.70% and 103.82 ± 4.04% with 2.49% and 3.90% RSD values, respectively. These results indicate the good application prospect of the ratiometric electrochemical sensing platform based on WP6@Fc-MOL.

Table 1 Determination results of Trp in milk samples by using Nafion/WP6@Fc-MOL/GCE electrode

Samples	Added (μM)	Found (μM)	RSD (%)	Recover (%)
Milk	20	21.60 ± 0.54	2.49	108.25 ± 2.70
	30	31.20 ± 1.21	3.90	103.82 ± 4.04

Conclusions

In conclusion, a ratiometric electrochemical sensing platform based on Fc and WP6 hybrid MOLs was developed, in which the ultrathin structure of MOLs provides more accessible active sites for the hybrid systems. Fc, as an interior label, can not only reduce the interference of other factors but also increase the electron transfer efficiency during the sensing process. WP6 could increase the selectivity of Trp based on host–guest interaction. The resulting electrode based on WP6@Fc-MOL possessed satisfactory ratiometric electrochemical sensing ability for Trp. These results indicate that this ratiometric electrochemical sensing platform can enhance the stability and accuracy for Trp sensing. Therefore, this work provides a good example of the rational design of supramolecular hybrid systems based on MOLs for ratiometric electrochemical detection.

Author contributions

J. Wen, W. Li and K. Yang conceived the idea and supervised the research. Z. Wu, J. Wen and K. Yang designed the study and developed the project. Z. Wu, J. Li, W. Zhang and Y. Li performed the experiments. Z. Wu, J. Li, J. Wen and K. Yang analyzed the data. Z. Wu, J. Wen and K. Yang wrote the paper with all authors reviewing the manuscript and providing feedback on the manuscript.

Conflicts of interest

There are no conflicts to declare.

Acknowledgements

This work was financially supported by the Natural Science Foundation of Hebei Province (No. B2020201043), the Advanced Talents Incubation Program of Hebei University (No. 521000981343 and 521000981345).

Notes and references

1 G. Wu, *Amino Acids*, 2009, **37**, 1–17.
2 M. O. Klein, D. S. Battagello, A. R. Cardoso, D. N. Hauser, J. C. Bittencourt and R. G. Correa, *Cell. Mol. Neurobiol.*, 2019, **39**, 31–59.
3 N. Sauer, R. Mosenthin and E. Bauer, *Nutr. Res. Rev.*, 2011, **24**, 46–59.
4 M. Wei, Y. Qiao, H. Zhao, J. Liang, T. Li, Y. Luo, S. Lu, X. Shi, W. Lu and X. Sun, *Chem. Commun.*, 2020, **56**, 14553–14569.
5 T. B. Wei, J. F. Chen, X. B. Cheng, H. Li, B. B. Han, Y. M. Zhang, H. Yao and Q. Lin, *Org. Chem. Front.*, 2017, **4**, 210–213.
6 J. Li, J. Jiang, Z. Xu, M. Liu, S. Tang, C. Yang and D. Qian, *Electrochim. Acta*, 2018, **260**, 526–535.
7 C. Liu, X. Wei, X. Wang, J. Shi, Z. Chen, H. Zhang, W. Zhang and X. Zou, *Sens. Actuators, B*, 2021, **329**, 129228.
8 H. Jin, R. Gui, J. Yu, W. Lv and Z. Wang, *Biosens. Bioelectron.*, 2017, **91**, 523–537.
9 X. Wang, G. Liu, Y. Qi, Y. Yuan, J. Gao, X. Luo and T. Yang, *Anal. Chem.*, 2019, **91**, 12006–12013.
10 Y. B. Huang, J. Liang, X. S. Wang and R. Cao, *Chem. Soc. Rev.*, 2017, **46**, 126–157.
11 J. Yang, C. Zhang, Y. Niu, J. Huang, X. Qian and K.-Y. Wong, *Chem. Eng. J.*, 2021, **409**, 128293.
12 J. Huang, X. Qian, J. Yang, Y. Niu, C. Xu and L. Hou, *Electrochim. Acta*, 2020, **340**, 135949.
13 H. Liu, X. Qian, Y. Niu, M. Chen, C. Xu and K.-Y. Wong, *Chem. Eng. J.*, 2020, **383**, 123129.
14 Y. Wang, H. Jin, Q. Ma, K. Mo, H. Mao, A. Feldhoff, X. Cao, Y. Li, F. Pan and Z. Jiang, *Angew. Chem., Int. Ed.*, 2020, **59**, 4365–4369.
15 T. Ma, H. Li, J. G. Ma and P. Cheng, *Dalton Trans.*, 2020, **49**, 17121–17129.
16 Z. Luo, S. Fan, C. Gu, W. Liu, J. Chen, B. Li and J. Liu, *Curr. Med. Chem.*, 2019, **26**, 3341–3369.
17 L. Cao, T. Wang and C. Wang, *Chin. J. Chem.*, 2018, **36**, 754–764.
18 L. Cao and C. Wang, *ACS Cent. Sci.*, 2020, **6**, 2149–2158.
19 Y. Quan, W. Shi, Y. Song, X. Jiang, C. Wang and W. Lin, *J. Am. Chem. Soc.*, 2021, **143**, 3075–3080.
20 X. Ling, D. Gong, W. Shi, Z. Xu, W. Han, G. Lan, Y. Li, W. Qin and W. Lin, *J. Am. Chem. Soc.*, 2021, **143**, 1284–1289.
21 G. T. Nash, T. Luo, G. Lan, K. Ni, M. Kaufmann and W. Lin, *J. Am. Chem. Soc.*, 2021, **143**, 2194–2199.
22 G. Lan, K. Ni, E. You, M. Wang, A. Culbert, X. Jiang and W. Lin, *J. Am. Chem. Soc.*, 2019, **141**, 18964–18969.
23 Y. Guo, W. Shi, H. Yang, Q. He, Z. Zeng, J. Y. Ye, X. He, R. Huang, C. Wang and W. Lin, *J. Am. Chem. Soc.*, 2019, **141**, 17875–17883.
24 J. Duan, S. Chen and C. Zhao, *Nat. Commun.*, 2017, **8**, 15341.
25 L. Yang, L. Cao, R. Huang, Z.-W. Hou, X.-Y. Qian, B. An, H.-C. Xu, W. Lin and C. Wang, *ACS Appl. Mater. Interfaces*, 2018, **10**, 36290–36296.
26 T. Ogoshi, T. A. Yamagishi and Y. Nakamoto, *Chem. Rev.*, 2016, **116**, 7937–8002.
27 M. Xue, Y. Yang, X. Chi, Z. Zhang and F. Huang, *Acc. Chem. Res.*, 2012, **45**, 1294–1308.
28 S. Cao, L. Zhou, C. Liu, H. Zhang, Y. Zhao and Y. Zhao, *Biosens. Bioelectron.*, 2021, **181**, 113164.
29 J. Zhou, M. Chen, J. Xie and G. Diao, *ACS Appl. Mater. Interfaces*, 2013, **5**, 11218–11224.
30 I. Hod, W. Bury, D. M. Gardner, P. Deria, V. Roznyatovskiy, M. R. Wasielewski, O. K. Farha and J. T. Hupp, *J. Phys. Chem. Lett.*, 2015, **6**, 586–591.
31 K. Yang, K. Yang, S. Chao, J. Wen, Y. Pei and Z. Pei, *Chem. Commun.*, 2018, **54**, 9817–9820.
32 Z. Wang, Y. Liu, Z. Wang, L. Cao, Y. Zhao, C. Wang and W. Lin, *Chem. Commun.*, 2017, **53**, 9356–9359.
33 G. Yu, M. Xue, Z. Zhang, J. Li, C. Han and F. Huang, *J. Am. Chem. Soc.*, 2012, **134**, 13248–13251.
34 L. Cao, Z. Lin, F. Peng, W. Wang, R. Huang, C. Wang, J. Yan, J. Liang, Z. Zhang, T. Zhang, L. Long, J. Sun and W. Lin, *Angew. Chem., Int. Ed.*, 2016, **55**, 4962–4966.
35 Y. Zhang, Z. Zhang, Z. Wang, H. Pan, Y. Lin and D. Chang, *Biosens. Bioelectron.*, 2021, **190**, 113437.
36 Y. M. Zhang, Q. Y. Yang, X. Q. Ma, H. Q. Dong, Y. F. Zhang, W. L. Guan, H. Yao, T. B. Wei and Q. Lin, *J. Phys. Chem. A*, 2020, **124**, 9811–9817.